The novel p.Ser263Phe mutation in the human high-affinity choline transporter 1 (CHT1/ *SLC5A7)* causes a lethal form of fetal akinesia syndrome.

Mayukh Banerjee*[,1], Denis Arutyunov*[,1], Daniel Brandwein[1], Cassandra Janetzki-Flatt[2], Hanna Kolski[4], Stacey Hume[2], Norma Jean Leonard[2,4], James Watt[4], Atilano Lacson[3], Monica Baradi[1], Elaine M. Leslie**[,1,3], Emmanuelle Cordat**[,1], Oana Caluseriu**[,2,4]

[1]Department of Physiology and Membrane Protein Disease Research Group, University of Alberta, Edmonton, Alberta, Canada

[2]Department of Medical Genetics, University of Alberta, Edmonton, Alberta, Canada

[3]Department of Laboratory Medicine and Pathology, University of Alberta, Edmonton, Alberta, Canada

[4]Department of Pediatrics, University of Alberta, Edmonton, Alberta, Canada

* These authors are joint first authors

** These authors are joint senior authors

Correspondence:

Oana Caluseriu, MD

Department of Medical Genetics

University of Alberta

e-mail: caluseri@ualberta.ca

Elaine M. Leslie, PhD

Department of Physiology

University of Alberta

e-mail: eleslie@ualberta.ca

Emmanuelle Cordat, PhD

Department of Physiology

University of Alberta

E-mail: cordat@ualberta.ca

Abstract

A subset of a larger and heterogeneous class of disorders, the congenital myasthenic syndromes (CMS) are caused by pathogenic variants in genes encoding proteins that support the integrity and function of the neuromuscular junction (NMJ). A central component of the NMJ is the sodium-dependent high-affinity choline transporter 1 (CHT1), a solute carrier protein (gene symbol *SLC5A7*), responsible for the reuptake of choline into the nerve termini has recently been implicated as one of several autosomal recessive causes of CMS. We report the identification and functional characterization of a novel pathogenic variant in *SLC5A7*, c.788C>T (p.Ser263Phe) in an El Salvadorian family with a lethal form of congenital myasthenic syndrome characterized by fetal akinesia. This study expands the clinical phenotype and insight into a form of fetal akinesia related to choline transporter defects and proposes a genotype-phenotype correlation for the lethal form of *SLC5A7*-related disorder with potential implications for genetic counseling.

Key words: congenital myasthenia syndrome, autosomal recessive, high-affinity choline transporter 1, *SLC5A7*, fetal akinesia syndrome

The neuromuscular junction (NMJ) is a complex structure that serves to efficiently communicate the electrical impulse from the motor neuron to the skeletal muscle to signal contraction (Hughes et al., (2006)). With the advent of next generation sequencing, several molecular causes of disorders of the NMJ have been deciphered over the past few years. Thirty genes acting at different levels in the NMJ define a growing class of disorders known as congenital myasthenic syndromes (CMS) (McMacken et al., (2017)). In addition to genetic heterogeneity, wide clinical heterogeneity is also observed in CMS. At the most severe end of the spectrum are lethal forms of the condition characterized by reduced intrauterine movement, postnatal severe generalized weakness, inability to maintain airways independently and a high rate of mortality.

Over the past few years, the discovery of a new autosomal recessive type 20 CMS (CMS20; OMIM# 617143) due to pathogenic variants in the choline transporter (CHT1) has included seven individuals (out of ten families) that survived with a clinical presentation ranging from arthrogryposis and hypotonia to treatable neonatal CMS with occasional apnea (Bauché et al., (2016); Wang et al., (2017); Pardal-Fernández et al., (2018)). In this group, two families presenting with a lethal phenotype were also described (**Supp**. **Table S1**) (Bauché et al., (2016); Wang et al., (2017)). An additional patient, who is possibly deceased, appears to have had a severe form of the disorder (**Supp. Table S1**) (Pardal-Fernández et al., (2018)). An autosomal dominant allelic form of CMS20 or distal hereditary motor neuropathy type VII (HMN-VII; OMIM 158580) with onset between the first and second decade of life was described in 2012 in an extensive pedigree (Barwick et al, 2012).

Homozygous *Slc5a7* knockout mice displayed irregular breathing, became cyanotic and died within one hour of birth (Ferguson et al., (2004)), a phenotype that closely resembles the lethal form of CHT1-related disorders previously reported in (Bauché et al., (2016); Wang et al., (2017); Pardal-Fernández et al., (2018)).

CHT1 is a glycoprotein belonging to the family of sodium-dependent glucose transporters (Okuda et al., (2000)). CHT1 is composed of 13 transmembrane helices, has an extracellular amino-terminus, cytosolic carboxy-terminus, and forms dimers/oligomers (Okuda et al., (2012)). The pathogenic variants reported by Bauché et al., and Wang et al., show a near complete loss of CHT1 function in cell models, which aligned with abnormal synaptic maturation or maintenance of the neuromuscular junction (Bauché et al., (2016); Wang et al., (2017)).

This report describes a new and severe CMS phenotype associated with a novel homozygous missense variant in the *SLC5A7* gene. This variant has only been reported to date in a heterozygous state in the gnomAD database (Lek et al., (2016)). Our functional studies confirm that the variant c.788C>T, encoding the substitution mutation p.Ser263Phe is associated with a total loss of CHT1 function, which explains the lethal phenotype observed in the patients.

Furthermore, we review the clinical presentation of the families with a lethal phenotype due to recessive mutations in the *SCL5A7* gene and propose a possible hypothesis for a phenotype-genotype correlation which will assist genetic counseling.

A Canadian consanguineous family of El Salvadorian ethnicity was evaluated in the neonatal period with a CMS-like disorder in two of their children, as shown in the pedigree (**Figure 1A**). The first child, who had displayed reduced prenatal movements, was a girl born at term who required resuscitation and was intubated following the delivery. She displayed profound generalized hypotonia, was ventilator-dependent, did not show dysmorphic features, but had arthrogryposis in all four limbs with no pterygia. The diagnostic work up for hypotonia showed a normal female chromosomal complement, and normal Prader Willi, spinal muscular atrophy, and myotonic dystrophy type 1 genetic testing. Nerve conduction studies/electromyography (EMG) were suggestive of a myasthenia gravis-like pattern (decrement with slow repetitive nerve stimulation). Further clinical genetic testing detailed in the Supplementary file was performed but as there was no clinical improvement with the use of pyridostigmine, 3,4-diaminopyridine, fluoxetine, and salbutamol, the family decided to withdraw care at 5 months of age. The second child had a neonatal presentation similar to his sister. Nerve conduction studies (**Supp. Figure S1A**) showed severe axonal motor and sensory polyneuropathy with neuromuscular junction dysfunction. A nerve biopsy showed primary axonopathy with giant axons and secondary myelin loss (**Supp. Figure S1B**). In absence of a response to pyridostigmine and with similarity with the sister's clinical presentation, withdrawal of care was decided at 1.5 months of age. Parents, who are first cousins once removed, were reportedly healthy with no congenital anomalies, no neurodevelopmental disorders or any motor restrictions. In the context of consanguinity with unaffected parents and two similarly affected children, the possibility of an autosomal recessive disorder was raised. A combination of SNP array based on identity by descent and exome sequencing of the two affected patients allowed the identification of a candidate gene, *SLC5A7* (See supplementary data for more information).

A homozygous variant was identified in *SLC5A7* (NM_021815.4, g. 108622551, c.788C>T, p.Ser263Phe) (**Figure 1A**). This transition from C to T in exon 7 substitutes a highly conserved nucleotide (phyloP 6.18 [-14.1;6.4]) and amino acid up to *C. elegans* (**Supp. Figure S2**). *In silico* analysis of c.788C>T, p.Ser263Phe using Alamut visual version 2.7, April 2015 (Interactive Biosoftware, Rouen, France) indicated this mutation to be probably damaging (Polyphen2, score 1.00, both HumVar and HumDiv), deleterious (score 0, SIFT), and disease causing (Align GVGD, classC65; score GV: 0.00, GD:154.81). This variant is present in gnomAD with an overall frequency of 0.00041% and 0.0030% in Latinos. Ser263 is predicted to be in the fourth cytosolic loop of CHT1 (**Figure 1B**). The variant reported here has been submitted to the ClinVar database (https://www.ncbi.nlm.nih.gov/clinvar/; submission ID: 111505).

The single nucleotide variant c.788C>T (p.Ser263Phe*)* was generated in the human CHT1-WT cDNA (gift from Randy Blakely (Addgene, plasmid # 15766) (Apparsundaram et al., (2000)) by site-directed mutagenesis as detailed in the Supplementary File. HEK293 cells stably expressing either empty vector, CHT1-WT or CHT1-Ser263Phe, were generated through selection of cells in G418 after a lentiviral infection process, as further detailed in the Supplementary File. To begin the characterization of CHT1-Ser263Phe and compare it to CHT1-WT, cell lysates from these cell lines at confluency were subjected to immunoblotting with anti-CHT1 rabbit polyclonal antibody (Supplementary File for further details). CHT1-WT and CHT1-Ser263Phe protein mobilities were compared. **Figure 1C** shows that in contrast to cells containing the empty vector, cell lysates expressing CHT1-WT displayed one band at around 70 kDa (black circle), an intermediate second band at a molecular weight consistent with the predicted 63 kDa (white circle) and a diffuse band with a slightly lower molecular weight (arrowhead) corresponding to 8 ± 4 % of the total CHT1 protein (n = 3, ± SD). Interestingly, we observed that total CHT1-Ser263Phe *(i)* was significantly less abundant than total WT-CHT1 (68 ± 7 % of WT-CHT1, n = 5, ± SD), and *(ii)* displayed the same three bands as the WT-CHT1, but the intensity of the top

band (black circle) significantly decreased from 46 ± 1 % in CHT1-WT to 33 ± 1 % in CHT1-Ser263Phe mutant (n = 3, ± SD).

The detection of multiple bands suggests that CHT1 is post-translationally modified possibly by carrying various forms of oligosaccharides, as suggested previously (Haga, (2014)). To determine if *N*-glycosylation was the reason for the different band mobilities, an enzymatic *N*-deglycosylation of the proteins in the lysate was performed with peptide-*N*-glycanase F (**Supp. Figure S3A**). Compared with mock digested samples (lane "-"), we observed a shift of the top bands to a lower molecular weight after digestion (arrowhead, lane "+"), supporting that CHT1 is *N*-glycosylated. The same pattern was observed for both CHT1-WT and CHT1-Ser263Phe, indicating that the glycosylation pattern is similar.

An alteration of the glycosylated/deglycosylated ratio as seen in **Figure 1C** might indicate abnormal processing of the CHT1-Ser263Phe compared with CHT1-WT. To address this possibility, HEK293 cells expressing CHT1-WT, CHT1-Ser63Phe or empty vector were immunostained with rabbit anti-CHT1 polyclonal antibody (Supplementary File for further details). CHT1-WT and CHT1-Ser263Phe were both detected in their respective cells and predominantly showed perinuclear staining (**Supp. Figure S3B**), indicative of intracellular localization. No obvious difference in localization was observed between the two proteins.

To further determine whether there was a difference in plasma membrane targeting, we conducted cell surface biotinylation experiments using a membrane impermeant biotinylation reagent (**Figure 1D**).This was done as described previously (Banerjee et al., (2016)), with minor modifications as detailed in the Supplementary File. Despite loading the same amount of total protein per lane (2.5 µg) and consistent with **Figure 1C & Supp Figure S3A**, CHT1-Ser263Phe displayed less intense bands, with a more intense low molecular weight band (white circle) compared with CHT1-WT. The unbound and biotinylated fractions of the mutant also displayed bands for the mutant that corresponded to 57 ± 4 % and 36 ± 19 % of the WT protein (n = 3, ± SD), respectively (**Figure 1E**). These results indicate that although the mutant was less

abundantly expressed in HEK293 cells, it reached the plasma membrane to the same extent as WT-CHT1 when corrected for protein level, providing further evidence that plasma membrane targeting of CHT1 is not affected by the p.Ser263Phe alteration.

As CHT1-Ser263Phe is able to reach the plasma membrane, we measured its functional activity using a [^{3}H]-choline uptake assay, based on a previously described method (Okuda and Haga, (2003)) with modifications as detailed in the Supplementary File. We compared the ability of HEK293 cells expressing either the empty vector, CHT1-WT or CHT1-Ser263Phe to transport [^{3}H]-choline (0.1 µM, 100 nCi) for up to 20 minutes (**Figure 2A, left panel**), and transport was quantified as described in the Supplementary File. In contrast with the CHT1-WT protein, which accumulated [^{3}H]-choline over the time course (linear up to 10 minutes), the mutant displayed a low transport activity that was similar to cells expressing the empty vector. This result indicates that CHT1-Ser263Phe is not able to transport choline at this single concentration. To further assess the function of the mutant, we measured its transport activity over multiple concentrations of [^{3}H]-choline. As shown in **Figure 2A (right panel)**, in contrast with the CHT1-WT that transported significantly more [^{3}H]-choline with increasing concentrations than cells with the empty vector, CHT1-Ser263Phe had a transport activity that did not differ from empty vector cells. Therefore, despite being present at the cell surface, CHT1-Ser263Phe transport of [^{3}H]-choline was not detected (**Figure 2A**).

We next determined whether we could restore the activity of the mutant protein at the plasma membrane. We incubated confluent HEK293 cells stably expressing either empty vector, CHT1-WT or CHT1-Ser263Phe with various chemical chaperones [C3 (kind gift from Dr. Gergely Lukacs, McGill University), VX809 (Selleckchem) or DMSO] (Brown et al., (1996); Van Goor et al., (2006), (2011)) or the proteasome inhibitor MG132 for 24 hours, at the indicated concentrations. CHT1 expression, cell surface abundance and activity were then examined. Chemical chaperones such as C3 and VX809 did not greatly increase the total abundance of CHT1-Ser263Phe although they increased CHT1-WT abundance (**Figure 2B**), therefore these

chaperones were not further examined. The MG132 incubation stabilized the unglycosylated form (arrowhead) and high molecular weight aggregates of the mutant (star), but did not increase the abundance of complex-glycosylated protein. DMSO treatment significantly increased the total abundance of both CHT1-WT and CHT1-Ser263Phe by 49% and 42%, respectively, compared to the untreated samples (**Figure 2C, lanes 1-4 & 2D**). Further, the cell surface abundance of CHT1-Ser263Phe was no longer significantly different from untreated CHT1-WT samples, indicating that DMSO treatment rescued both the abundance and cell surface expression of the mutant. The rescuing effect of DMSO on CHT1-Ser263Phe transport activity was assessed next. As shown in **Figure 2E**, despite the increased level of CHT1-Ser263Phe at the cell surface, the transport activity was not rescued by 1% DMSO incubation as it remained similar to cells expressing the empty vector. These results show that although DMSO increased the total and cell surface expression of the mutant, it did not improve the functional defect induced by the substitution of serine 263 to phenylalanine.

In this manuscript, we report the characterization of a novel missense substitution within the CHT1 protein that caused a lethal form of fetal akinesia syndrome. The family studied presented at the most severe end of the spectrum seen in congenital myasthenic syndrome type 20 due to impaired cholinergic signaling (OMIM 617143). The p.Ser263Phe missense variant involves a highly conserved residue of the CHT1 protein in the fourth cytoplasmic loop, and all *in silico* analyses deemed the variant pathogenic or disease-causing. Stable expression of CHT1-WT or CHT1-Ser263Phe in HEK293 cells allowed us to characterize the behavior of this mutant. The mutant was found to migrate on SDS-PAGE gel as three main bands, however, the different ratio of complex glycosylated/high mannose glycosylated/deglycosylated protein seen in WT and mutant CHT1 suggests different intracellular processing for the two proteins. Indirect immunofluorescence showed similar localization for both the WT and Ser263Phe-CHT1 mutant, with predominant intracellular localization and minimal staining at the plasma membrane (Supp. **Figure S3B**). Our WT-CHT1 staining differs from that shown by Bauché and colleagues (Bauché

et al., (2016)), but is however consistent with previous findings supporting the presence of CHT1 in early and recycling endosomes with 90% of the protein residing in intracellular vesicles at the neuromuscular junction (Nakata et al., (2004); Ribeiro et al., (2006), (2007)). Nevertheless, the transport results confirmed that CHT1-WT was present at the plasma membrane and transported significant amounts of choline (**Figure 2A**). In contrast, CHT1-Ser263Phe did not have detectable choline uptake activity, despite its presence at the cell surface (**Figure 1D, 1E, & 2A**). The increased expression and cell surface trafficking of CHT1-Ser263Phe variant in the presence of DMSO (**Figure 2C-2E**) indicates that some chemical chaperones may potentially be used to rescue low expressing but functional CHT1 mutants. Interestingly, Choudhary and colleagues recently examined a library of 2,753 small molecules from Pfizer Chemogenomic Library and 880 additional compounds for their potential beneficial effect on CHT1 biology. These authors identified 4 compounds that acted as positive modulators of CHT1 (Choudhary et al., (2017)). Some of these compounds may have a rescuing effect on the inactive CHT1-Ser263Phe and/or other naturally occurring CHT1 variants.

The loss of function of CHT1 due to a substitution of serine at codon 263 with a phenylalanine could have multiple explanations. The hydroxyl group of the serine could be important for CHT1 function or the bulky and hydrophobic phenylalanine could disrupt function. The cytosolic Ser263 may be phosphorylated, which could in turn affect the transport activity of CHT1. Previous studies have shown that activating protein kinase C or inhibiting protein phosphatases 1/2A affect the cell surface abundance and consequently the function of CHT1 in mouse and rat striatal and hippocampal synaptosomes, and that CHT1 is phosphorylated (Issa et al., (1996); Cooke and Rylett, (1997); Gates et al., (2004); Black et al., (2010)). More recently, the CXCL12 chemokine was shown to up-regulate CHT1 in an Akt-mediated process in rat pheochromocytoma PC-12 cells and rat primary neuronal cultures (Yan et al., (2016)). However, the phosphorylation site(s) on CHT1 responsible for this has (have) not been identified.

Our family is the fourth reported in the literature with a lethal phenotype of myasthenic syndrome suggesting an overlap with fetal akinesia syndromes. Three of the families with lethal presentation, including the one described by us, have had two affected offspring each that have demonstrated high penetrance and homogeneity of the clinical condition (Supp. **Table S1**). While 15 missense mutations have been described to date (Bauché et al., (2016); Wang et al., (2017); Pardal-Fernández et al., (2018)), the four families with a lethal phenotype are either homozygous for a missense mutation (Family 2 in Wang et al, 2017, patient described by Pardal-Fernandez et al, 2018 and our family) or have a combination of a missense and a nonsense mutation (Family 2 in Bauché et al, 2016). We observed that location of the mutations leading to lethal outcomes, in our family as well as Family 2 in Wang et al, 2017 and Family 2 in Bauché et al, 2016 are consistently located in the cytosolic domain of CHT1 (**Figure 1B**). However, the patient described by Pardal-Fernandez and assumed to be demised based on their description, carried two missense mutations: one in transmembrane domain 13, and a second in the fifth extracellular loop (**Figure 1B**). The CHT1 amino acid mutated in our family, serine 263, is located at the beginning of the fourth cytosolic loop between transmembrane domains 7 and 8 according to the topological model from Okuda and colleagues (**Figure 1B**) (Okuda and Haga, (2003)). Based on the information to date, it is difficult to infer a genotype-phenotype correlation for the patients presenting with lethality compared to patients that survived and responded to treatment and this remains an important question to be answered by future studies. All the cases surviving beyond the neonatal or early childhood timeframe were compound heterozygous for missense variants with at least one variant in the transmembrane domain. Three of the families with a lethal phenotype, described by Bauché et al. (2016), Wang et al. (2017) and our family, have pathogenic substitutions in the cytosolic portion of the protein and demonstrate a loss of function despite significant proper plasma membrane targeting. Possible explanations for the phenotype in our family in relation to a cytosolic residue interfering with choline transport include an impairment of: *(i)* choline release into the cytosol, *(ii)* post-translational modifications (including potential

phosphorylation), *(iii)* regulatory protein:protein interactions, and *(iv)* additive effects of multiple polymorphisms present in genes involved in NMJ function. However, these suggestions need further study and the topological model requires further validation.

An explanation for the recessive nature of the CHT1-Ser263Phe and thus absence of symptoms in the parents of the families described with CMS20 remains speculative. As CHT1 is known to form homodimers (Okuda et al., (2012)), it is likely that heterodimers formed of one WT allele and one mutated allele are less functional, but enough to maintain sufficient choline transport at the neuromuscular junction which is supported by the lack of reported motor issues by both parents of our family who are in their 40's. C-terminal truncating mutations of *SLC5A7* are known to cause late onset dominant hereditary motor neuropathies, through a dominant negative effect of the truncated CHT1 on WT-CHT1 levels and targeting to the cell surface (Barwick et al., (2012); Salter et al., (2018)). In Family 2 from Bauché et al, one parent is heterozygous for a nonsense mutation in the N-terminal part of the protein, I42*, expected to produce a truncated form of the protein possibly followed by non-sense mediated decay rather that a dominant negative effect on the WT allele (Bauché et al., (2016)). No comments are made on a possible phenotypic effect on any of the parents of the autosomal recessive cases described to date. However, why certain CHT1 mutations have dominant versus recessive effects requires further investigation. Understanding a genotype-phenotype correlation between the clinical presentation and the underlying pathophysiologic mechanism could have a direct impact on counseling of families with similar pathogenic variants in relation to prognosis and anticipatory management, especially for cases diagnosed in the prenatal or neonatal time.

Interestingly, in our family, the nerve biopsy from one patient (Patient 2) indicates the presence of enlarged axons and reduced myelin (Supp. **Figure S1B**). Myelination is a process that continues after birth, however, this reduced level of myelin was unexpected. Cholesterol is an important constituent of the myelin (Deber and Reynolds, (1991)). Evidence suggests a critical and direct relation between the integrity of lipid rafts in plasma membrane and CHT1 function and localization (Cuddy et al., (2014)). It would be interesting to understand if this observation of reduced myelination in our patients with homozygous CHT1 pathogenic variants is supported in

additional families. A nerve biopsy was not available for comparison between the two allelic disorders CMS20 and HMN7A (Barwick et al., (2012)). Our observation regarding defective myelination in the recessive form of the *SLC5A7*-related disorder could suggest that pathogenicity of CHT1 variants is not limited strictly to the transport of choline but may also influence myelination with a combined functional effect.

Interestingly, the c.788C>T substitution is reported in a *SLC5A7* carrier of Hispanic descent in the gnomAD database, suggesting that the C788T mutation may be a recurrent variation found in a subpopulation of individuals of this ethnic background. This finding underlines the importance of functional characterization of DNA variants for recessive traits present in databases of typical individuals.

Acknowledgements

We thank the family for their invaluable participation to this study. This project was supported by the British Columbia Rare Disease Foundation (OC), Women's and Children's Health Research Institute at the University of Alberta Innovation (RES0018693; OC) and seed grant (RES0027086; OC, EC, EL, MB), and Branch Out Neurology Foundation (CJF). MB was partially supported by an Alberta Cancer Foundation Cancer Research Postdoctoral Fellowship award and Women's and Children's Health Research Institute at the University of Alberta seed grant. EML was an Alberta Innovates Health Solutions Scholar. Canadian Institutes of Health Research operating grants supported DA (MOP 142251) and MB (MOP 272075).

References

Apparsundaram S, Ferguson SM, George AL, Blakely RD. (2000). Molecular Cloning of a Human, Hemicholinium-3-Sensitive Choline Transporter. *Biochemical and Biophysical Research Communications* **276**:862–867.

Banerjee M, Marensi V, Conseil G, Le XC, Cole SPC, Leslie EM. (2016). Polymorphic variants of MRP4/ABCC4 differentially modulate the transport of methylated arsenic metabolites and

physiological organic anions. *Biochemical Pharmacology* **120**:72–82

Barwick KES, Wright J, Al-Turki S, McEntagart MM, Nair A, Chioza B, Al-Memar A, Modarres H, Reilly MM, Dick KJ, Ruggiero AM, Blakely RD, Hurles ME, Crosby AH.(2012). Defective Presynaptic Choline Transport Underlies Hereditary Motor Neuropathy. *Am J Hum Genet* 91:1103-1107.

Bauché S, O'Regan S, Azuma Y, Laffargue F, McMacken G, Sternberg D, Brochier G, Buon C, Bouzidi N, Topf A, Lacène E, Remerand G, et al. (2016). Impaired Presynaptic High-Affinity Cholne Transporter Causes a Congenital Myasthenic Syndrome with Episodic Apnea *Am J of Hum Genet* **99**:753-61.

Black SAG, Ribeiro FM, Ferguson SSG, Rylett RJ. (2010). Rapid, transient effects of the protein kinase C activator phorbol 12-myristate 13-acetate on activity and trafficking of the rat high-affinity choline transporter. *Neuroscience* **167**:765–773.

Brown CR, Hong-Brown LQ, Biwersi J, Verkman AS, Welch WJ. (1996). Chemical chaperones correct the mutant phenotype of the delta F508 cystic fibrosis transmembrane conductance regulator protein. *Cell stress & chaperones* **1**:117–25.

Choudhary P, Armstrong EJ, Jorgensen CC, Piotrowski M, Barthmes M, Torella R, Johnston SE, Maruyama Y, Janiszewski JS, Storer RI, Skerratt SE, Benn CL. (2017). Discovery of Compounds that Positively Modulate the High Affinity Choline Transporter. *Frontiers in Molecular Neuroscience* **10**:40.

Cooke LJ, Rylett RJ. (1997). Inhibitors of serine/threonine phosphatases increase membrane-bound choline acetyltransferase activity and enhance acetylcholine synthesis. *Brain research* **751**:232–8.

Cuddy LK, Winick-Ng W, Rylett RJ. (2014). Regulation of the high-affinity choline transporter activity and trafficking by its association with cholesterol-rich lipid rafts. *Journal of neurochemistry* **128**:725–40.

Deber CM, Reynolds SJ. (1991). Central nervous system myelin: structure, function, and

pathology. *Clinical biochemistry* **24**:113–34.

Ding Q, Shen D, Dai Y, Hu Y, Guan Y, Liu M, Cui L. (2018). Mechanism hypotheses for the electrophysiological manifestations of two cases of endplate acetylcholinesterase deficiency related congenital myasthenic syndrome. *Journal of Clinical Neuroscience* **48**:229–232.

Ferguson SM, Bazalakova M, Savchenko V, Tapia JC, Wright J, Blakely RD. (2004). Lethal impairment of cholinergic neurotransmission in hemicholinium-3-sensitive choline transporter knockout mice. *Proceedings of the National Academy of Sciences* **101**:8762–8767.

Gates J, Ferguson SM, Blakely RD, Apparsundaram S. (2004). Regulation of Choline Transporter Surface Expression and Phosphorylation by Protein Kinase C and Protein Phosphatase 1/2A. *Journal of Pharmacology and Experimental Therapeutics* **310**:536–545.

Goor F Van, Hadida S, Grootenhuis PD, Burton B, Stack JH, Straley KS, Decker CJ, Miller M, McCartney J, Olson ER, Wine JJ, Frizzell RA, et al. (2011). Correction of the F508del-CFTR protein processing defect in vitro by the investigational drug VX-809. *Proc Natl Acad Sci U S A* **108**:18843–18848.

Goor F Van, Straley KS, Cao D, González J, Hadida S, Hazlewood A, Joubran J, Knapp T, Makings LR, Miller M, Neuberger T, Olson E, et al. (2006). Rescue of ΔF508-CFTR trafficking and gating in human cystic fibrosis airway primary cultures by small molecules. *American Journal of Physiology-Lung Cellular and Molecular Physiology* **290**:L1117–L1130.

Haga T. (2014). Molecular properties of the high-affinity choline transporter CHT1. *The Journal of Biochemistry* **156**:181–194.

Hantai D, Nicole S, Eymard D.(2013). Congenital myasthenic syndromes: an update. *Curr Opin Neurol* 26:561-568

Hughes BW, Kusner LL, Kaminski HJ. (2006). Molecular architecture of the neuromuscular junction. *Muscle & nerve* **33**:445–61.

Issa AM, Gauthier S, Collier B. (1996). Effects of the phosphatase inhibitors calyculin A and okadaic acid on acetylcholine synthesis and content of rat hippocampal formation. *Journal of*

neurochemistry **66**:1924–32.

Lek M, Karczewski KJ, Minikel E V, Samocha KE, Banks E, Fennell T, O'Donnell-Luria AH, Ware JS, Hill AJ, Cummings BB, Tukiainen T, Birnbaum DP, et al. (2016). Analysis of protein-coding genetic variation in 60,706 humans. *Nature* **536**:285–91.

McMacken G, Abicht A, Evangelista T, Spendiff S, Lochmüller H. (2017). The Increasing Genetic and Phenotypical Diversity of Congenital Myasthenic Syndromes. *Neuropediatrics* **48**:294–308.

Nakata K, Okuda T, Misawa H. (2004). Ultrastructural localization of high-affinity choline transporter in the rat neuromuscular junction: Enrichment on synaptic vesicles. *Synapse* **53**:53–56.

Okuda T, Haga T. (2003). High-affinity choline transporter. *Neurochemical research* **28**:483–8.

Okuda T, Haga T, Kanai Y, Endou H, Ishihara T, Katsura I. (2000). Identification and characterization of the high-affinity choline transporter. *Nature Neuroscience* **3**:120–125.

Okuda T, Osawa C, Yamada H, Hayashi K, Nishikawa S, Ushio T, Kubo Y, Satou M, Ogawa H, Haga T. (2012). Transmembrane topology and oligomeric structure of the high-affinity choline transporter. *J Biol Chem* **287:**42826-42834.

Omasits U, Ahrens CH, Müller S, Wollscheid B. (2014). Protter: interactive protein feature visualization and integration with experimental proteomic data. *Bioinformatics* **30**:884–886.

Pardal-Fernández JM, Carrascosa-Romero MC, Álvarez S, Medina-Monzón MC, Caamaño MB, Cabo C de. (2018). A new severe mutation in the *SLC5A7* gene related to congenital myasthenic syndrome type 20. *Neuromuscular Disorders* **28**:881–884.

Ribeiro FM, Black SAG, Prado VF, Rylett RJ, Ferguson SSG, Prado MAM. (2006). The "ins" and "outs" of the high-affinity choline transporter CHT1. *Journal of Neurochemistry* **97**:1–12.

Ribeiro FM, Pinthong M, Black SAG, Gordon AC, Prado VF, Prado MAM, Rylett RJ, Ferguson SSG. (2007). Regulated recycling and plasma membrane recruitment of the high-affinity choline transporter. *European Journal of Neuroscience* **26**:3437–3448.

Salter CG, Beijer D, Hardy H, Barwick KES, Bower M, Mademan I, De Jonghe P, Deconinck T, Russell MA, McEntagart MM, Chioza BA, Blakely RD, Chilton JK, De Bleecker J, Baets J, Baple EL, Walk D, Crosby AH. (2018). Truncating SLC5A7 mutations underlie a spectrum of dominant hereditary motor neuropathies. *Neurol Genet* **4:**e222.

Wang H, Salter CG, Refai O, Hardy H, Barwick KES, Akpulat U, Kvarnung M, Chioza BA, Harlalka G, Taylan F, Sejersen T, Wright J, et al. (2017). Choline transporter mutations in severe congenital myasthenic syndrome disrupt transporter localization. *Brain* **140**:2838–2850.

Yan J, Zhao W, Guo M, Han X, Feng Z. (2016). CXCL12 Regulates the Cholinergic Locus and CHT1 Through Akt Signaling Pathway. *Cellular Physiology and Biochemistry* **40**:982–992.

Figure Legends

Figure 1. A, Autosomal recessive pedigree of our study family with the corresponding Sanger sequencing electropherograms for the c.788C>T. Consanguineous parents are carriers. One male offspring is unaffected. One male and one female offspring were affected, required ventilation at birth and died at 2 and 5 months, respectively. Children displayed lack of prenatal movement, postnatal difficulties breathing and sucking and progressive muscle weakness. **B**, SLC5A7 topological model and location of mutations reported to date. Red circles and arrows: all mutations in patients with lethal form of the condition are located in the intracytoplasmic domain- see text for details; black circles: mutations in viable patients; branches represent predicted N-glycosylation sites. Note: There are viable patients who are combined heterozygous with one mutation in the intracellular domain and one in the transmembrane domain. The topology plot was generated using Protter 1.0 Software (Omasits et al., (2014)). C, Immunoblot of HEK293 cells stably expressing the empty vector (EV), CHT1-WT or CHT1-S263FSer263Phe. C and D, Black circle indicates CHT1 carrying complex oligosaccharide, white circle shows core

glycosylated CHT1, arrowhead indicates unglycosylated CHT1. D, Cell surface biotinylation of cells expressing the empty vector, CHT1-WT or -S263FSer263Phe. The membranes were blotted with anti-CHT1 (top blot), anti-GAPDH (middle blot) or anti-Na+/K+-ATPase (bottom blot) antibodies. Lack of GAPDH in the biotinylated fraction shows that the membrane impermeant biotin reagent did not leak intracellularly and the Na+/K+-ATPase was chosen as a positive control for the biotinylation. E, Quantification of total (input), unbound and cell surface CHT1-S263FSer263Phe relative to CHT1-WT indicating that the mutant is less abundant at the plasma membrane, but not significantly different when corrected for input level. Error bars correspond to means ± SD, n=3. **P < 0.01, ***P < 0.001 versus "WT" condition using one-way ANOVA with Dunett's Multiple Comparisons post-hoc test.

Figure 2. **A**, Transport of [3H]-choline by HEK293 cells stably expressing CHT1-WT or CHT1-Ser263Phe. Left panel, single concentration [3H]-choline (0.1 μM) transport assay over 20 minutes; right panel, multiple concentrations of [^{3}H]-choline (0.1, 2.5 and 10.0 μM) and a single time point of 5 minutes. Error bars correspond to means ± SD, n=3. **P < 0.01, ***P < 0.001 versus "empty vector" condition using one-way ANOVA with Dunnett's Multiple Comparisons post-hoc test. Results from cells expressing CHT1-Ser263Phe were not significantly different from empty vector expressing cells. **B**, Immunoblot from HEK293 cells expressing CHT1-WT or CHT1-Ser263Phe either untreated or after incubation with various amounts of chemical chaperones (C3, VX809) or the proteasome inhibitor MG132 for 24 hours. Numbers below the blot indicate the percentage of mutant protein expression relative to untreated condition. Black circle indicates CHT1 carrying complex oligosaccharides, white circle shows core glycosylated CHT1, arrowhead indicates unglycosylated CHT1, # signs shows a band non-specifically recognized by the antibody. **C**, Cell surface biotinylation of HEK293 cells expressing either WT- or Ser263Phe-CHT1 and untreated or incubated with 1% DMSO for 24 hours. Black circle indicates CHT1 carrying complex oligosaccharides, white circle shows core glycosylated CHT1, arrowhead indicates

unglycosylated CHT1. **D**, Quantification of total, unbiotinylated and biotinylated WT- or Ser263Phe- CHT1 with and without DMSO treatment. Error bars correspond to means ± SD, n=3. *P < 0.05, **P < 0.01 versus “untreated CHT1-WT” condition using one-way ANOVA with Dunnett’s Multiple Comparisons post-hoc test. **E**, Choline transport measured from HEK293 cells expressing empty vector, WT- or Ser263Phe-CHT1 and either kept untreated or incubated with 1% DMSO for 24 hours. Error bars correspond to means ± SD, n=3. *P < 0.05 versus “vector” condition using one-way ANOVA with Dunnett’s Multiple Comparisons post-hoc test.

The novel p.Ser263Phe mutation in the human high-affinity choline transporter 1 (CHT1/ *SLC5A7)* causes a lethal form of fetal akinesia syndrome.

Mayukh Banerjee*[,1], Denis Arutyunov*[,1], Daniel Brandwein[1], Cassandra Janetzki-Flatt[2], Hanna Kolski[4], Stacey Hume[2], Norma Jean Leonard[2,4], James Watt[4], Atilano Lacson[3], Monica Baradi[1], Elaine M. Leslie**[,1,3], Emmanuelle Cordat**[,1], Oana Caluseriu**[,2,4]

Supplementary Files

Detailed Materials and Methods

The Family

A Canadian consanguineous family of El Salvadorian ethnicity was evaluated in the neonatal period and found to have the same CMS-like disorder in two of their children, as shown in the pedigree (Figure 1A). The children displayed reduced prenatal movements, and arthrogryposis with elbow, wrist, and knee flexion, no pterygia and camptodactyly diagnosed at birth. The first child was a girl born at term who required resuscitation and intubation following the delivery. The diagnostic work up for hypotonia showed a normal female chromosomal complement, and normal genetic testing for Prader Willi, spinal muscular atrophy, and myotonic dystrophy type 1. There was a normal electroencephalogram (EEG), no structural brain anomalies on MRI, and nerve conduction studies/electromyography (EMG) were suggestive of a myasthenia gravis-like pattern (decrement with slow repetitive nerve stimulation). Further clinical genetic testing available at the time showed no pathogenic variants in the rapsyn, alpha and epsilon subunits of the acetylcholine receptor gene, and the COLQ gene by sequencing. She remained areflexic, with profound hypotonia, and was ventilator dependent (requiring supplemental manual ventilation due to acute episodes of decompensation). There was no clinical improvement with the use of pyridostigmine, 3,4-diaminopyridine, fluoxetine, and salbutamol. At 5 months of age, the family decided to withdraw care. Five years later, a brother was born at 36 weeks gestation following a pregnancy characterized by lack of fetal movements and polyhydramnios. His neonatal presentation was similar to his sister; he required neonatal resuscitation and was ventilator-dependent, had profound hypotonia and minimal muscle power against gravity. Nerve conduction studies (Supp. Figure S1A) showed severe axonal motor and sensory polyneuropathy with neuromuscular junction dysfunction, and brain MRI was normal. A nerve biopsy showed primary axonopathy with giant axons and secondary myelin loss (Supp. Figure S1B). A course of pyridostigmine did not improve his presentation. He had two rounds of aspiration pneumonia

and withdrawal of care was decided at 1.5 months of age. Parents were reportedly healthy with no congenital anomalies or neurodevelopmental disorders.

A single nucleotide polymorphism (SNP) clinical array was performed for the purpose of identifying areas of homozygosity shared by the two affected siblings. These were: hg19: 12q11q13.13 (chr 12:37857750-52353578); 19q13.11q13.41 (chr19:34168272-51640321); 2q11.1q14.1 (chr2:95341387-115179913); 3p21.31p21.1 (chr3:46726738-53002150); 9q21.13q21.32 (chr9:78190522-84727196). None of the 18 CMS genes known at the time, majority of them recessive, (Hantai, Nicole and Eymard and Lévyet al, (20132)) were located within the homozygosity regions identified. Further, the family was offered next generation sequencing studies on a research basis upon signing informed written consent approved by the University of Alberta human research ethics board (Protocol 00043169) for the unaffected parents, the affected children and an unaffected brother. At the end of the study, in view of additional CMS genes discovered in the meantime, the exome data obtained previously on the two affecteds was again screened for variants in all 30 genes reported (McMacken et al, 2017). A variable number of SNPs were identified in the majority of the genes in both patients, with the exception of a heterozygous MYO9A variant in patient 2, and a heterozygous COLQ splicing variant in patient 1. Of note, both MYO9A and COLQ are known to be responsible for autosomal recessive forms of CMS, and therefore these variants were not considered to contribute to the phenotype in our patients.

Whole exome sequencing studies

Genomic DNA from the two affected patients underwent whole exome sequencing (WES) performed by Macrogen Inc. using Agilent's SureSelect 51 Mb enrichment kit at 100X average on-target depth coverage. Sequencing was completed on an Illumina HiSeq 2000 using 100-bp paired-end sequencing method and a target coverage of 99%. The reads were mapped against UCSC hg19 (http://genome.ucsc.edu/), using BWA (http://bio-bwa.sourceforge.net/) and

SAMTOOLS (http://samtools.sourceforge.net/). The ~75 000 variants per patient were filtered as follows: minor allele frequency of 1% or higher in dbSNP135 and 1000 genome, and variants in the known CMS genes to date without an identified pathogenic variant. Subsequently, we proceeded to analyze data under an autosomal recessive model of inheritance by focusing the analysis on the regions of homozygosity identified by SNP array.

Site-directed mutagenesis

The human CHT1-WT cDNA was a gift from Randy Blakely (Addgene, plasmid # 15766) (Apparsundaram et al., (2000)). The single nucleotide variant c.788C>T (p.S263FSer263Phe) was generated by site-directed mutagenesis. Briefly, the human CHT1 cDNA was cloned into the pLVX-IRES-Hygromycin B (Hyg) vector (Clontech) using BamHI restriction sites flanking the CHT1 cDNA. After confirmation of the successful cloning by Sanger sequencing, the construct bearing human CHT1-wild-type (WT) cDNA was amplified using the Q5 site-directed mutagenesis kit (New England Biolabs) with mutagenic primers containing the desired variant (hCHT1 S263FSer263Phe Forward: AGG GTT CTC TTT TCT TCC TCA G; hCHT1 S263FSer263Phe Reverse: CTG AAA GTA TGC TTG CCA TG). The resulting cDNA was sequenced to confirm the presence of the variant (The Applied Genomics Core, University of Alberta, Edmonton, Canada).

Cell Culture

HEK293 cells (Clontech) were grown in complete medium [Dulbecco's Modified Eagle's Medium (DMEM) (Gibco) supplemented with 10% fetal bovine serum (FBS) (Sigma-Aldrich), 100 units/ml of penicillin and 100 µg/mL of streptomycin (ThermoFisher Scientific)] at 37°C in a humidified incubator with 5% CO2. To express human CHT1 in mammalian cells, we used a lentiviral infection process, followed by selection to obtain HEK293 cells stably expressing either CHT1-WT or CHT1-Ser263Phe. First, CHT1-WT or CHT1-Ser263Phe cDNA in pLVX-IRES-Hyg was transiently transfected in HEK293 cells using the single shot packaging kit (Clontech) and

the supernatant containing the viruses was collected 48 hours later. After filtering through a 0.45 µm filter, the cell supernatant was used to transduce new HEK293 cells in the presence of 8 µg/ml polybrene (Sigma) and CHT1-stably expressing cells were selected in complete growth medium supplemented with 0.2 mg/ml Hygromycin B (Thermo Scientific).

Immunoblot

Confluent HEK293 cells expressing CHT1-WT and CHT1-Ser263Phe were lysed in PBS containing 1% Triton X-100 and protease inhibitors [Complete^{TM} Mini EDTA-free (Roche)]. Total protein concentration was measured using the BCA (bicinchoninic acid) protein assay kit (Pierce). Total proteins (20 µg) were subjected to SDS-PAGE, transferred onto a PVDF membrane (Millipore) and membranes were then blocked with 3% skim milk powder (BioBasic) in Tris-buffered saline with 0.1 % Tween 20 (TBST) for 1 hr. Membranes were incubated with anti-CHT1 rabbit polyclonal antibody (ABN458, 1:2500) (Millipore) in TBST containing 1% skim milk followed by anti-rabbit HRP-conjugated secondary antibody (1:10,000) (GE Healthcare). Proteins on the blots were detected with Clarity Western chemiluminescent detection reagent (Bio-Rad) and bands visualized using ChemiDoc MP Imaging System (BioRad). Membranes were subsequently re-probed with monoclonal anti-mouse β-actin antibody (1:20,000, Origen) in 1% BSA TBST followed with HRP-conjugated anti-mouse secondary antibody (1:15,000, GE Healthcare) in 1% BSA TBST. Relative band intensities were determined using the freeware ImageLab (Bio-Rad).

For rescuing CHT1-Ser263Phe, 50% confluent cells were incubated with complete medium containing 0.2 mg/ml hygromycin and C3 (kind gift from Dr. Gergely Lukacs, McGill University), VX809 (Selleckchem) or DMSO at the indicated concentrations. Cells were subsequently grown for 24 hours at 37°C under standard conditions. Cells were then lysed on ice in PBS containing 1% Triton-X-100 (Fisher Scientific) and CompleteMini EDTA-free Protease Inhibitor Cocktail (Roche). Lysate protein concentrations were determined using a BCA Protein Assay kit (Pierce) and the samples were subjected to immunoblot, as described above.

Immunofluorescence

HEK293 cells expressing CHT1-WT, CHT1-Ser263Phe or empty vector were seeded on 6 well plates with poly-L-lysine coated coverslips. Cells were fixed with 4% paraformaldehyde in PBS, washed with PBS containing 100 mM glycine, permeabilized with 0.2% Triton X-100 in PBS, and blocked with 1% BSA in PBS. Coverslips were then incubated with rabbit anti-CHT1 polyclonal antibody (1:500, Millipore) in 1% BSA in PBS for 30 min, washed and incubated with goat anti-rabbit antibody conjugated with Alexa 488 (1:500, GE Healthcare) in 1% BSA in PBS. DAPI (Thermo Scientific) was used to stain nuclei. The coverslips were then mounted on slides with DAKO mounting solution. Image acquisition was done with an Olympus IX81 microscope equipped with a Nipkow spinning disk optimized by Quorum Technologies (Guelph, ON, Canada) and a 63X oil objective.

Cell surface biotinylation

HEK293 cells expressing CHT1-WT, CHT1-Ser263Phe or empty vector were seeded on 6 well plates. Forty-eight hours post-seeding, the cells were incubated with or without 1% DMSO in complete medium for 24 hours. The cells were subsequently subjected to cell surface biotinylation, as described previously (Banerjee et al., (2016)), with minor modifications. Following incubation with membrane impermeant EZ-Link biotinylation reagent (Thermo Scientific, Rockforl, IL) and lysis as described previously, total protein levels were measured. An aliquot of the lysate was saved (total fraction) and 450 µg of each lysate was subsequently incubated with 140 µL streptavidin beads for 1 hour on a rocker at 4°C. Following centrifugation, the supernatant was collected, and an aliquot kept as the unbiotinylated fraction. After washing, the beads were resuspended in 50 µL of 2X Laemmli buffer and incubated at room temperature for 30 min. The eluted biotinylated proteins were subsequently collected by centrifugation (biotinylated fraction) and 25 µl loaded for immunoblot along with 2.5 µg of total fraction and a matched volume of

unbound fraction per well. In addition to CHT1, the blots were probed for cytosolic GAPDH to ensure cell membrane integrity was intact during the biotinylation procedure [mouse monoclonal anti-GAPDH 6C5 (1:10,000) ; Santa Cruz Biotechnology, Dallas, TX], and for Na^+/K^+ATPase as a loading control [mouse monoclonal anti Na^+/K^+ATPase H-3 (1:10,000); Santa Cruz Biotechnology, Dallas, TX]. Since the Na^+/K^+ATPase is present in both the unbound and biotinylated fractions, each fraction was normalized for loading only within that particular fraction.

Choline uptake assay

HEK293 cells stably expressing empty vector, CHT1-WT or CHT1-Ser263Phe were seeded on poly-L-lysine coated 6 well plates at a density of 0.8 x 106 cells/well in a total volume of 2 ml. Choline uptake was measured based on a previously described method (Okuda and Haga, (2003)) with modifications. Briefly, after 48 hours, the cells were washed twice with 1.5 ml of warm (37°C) Krebs-Ringer's-HEPES (KRH) buffer (130 mM NaCl, 1.3 mM KCl, 2.2 mM $CaCl_2.2H_2O$, 1.2 mM $MgSO_4.7H_2O$, 1.2 mM KH_2PO_4, 10 mM HEPES, 10 mM glucose, pH 7.40). The cells were then pre-incubated at 37°C with KRH buffer for 10 minutes, next replaced with 1 ml of KRH containing [^{3}H]-choline (choline chloride, [methyl-^{3}H], 78.3 Ci/mmol, Perkin Elmer) (0.1, 2.5 or 10 µM, 100 nCi/ml) and incubated at 37°C for 5 min. Cells were next washed three-times with ice-cold KRH buffer and lysed using 750 µl of 1% SDS in water. Transport of [^{3}H]-choline was quantified using a liquid scintillation counter (Beckman model LS6000IC). Transport activity was normalized against the total protein concentration in each well.

For the time course experiment, cells were incubated with [^{3}H]-choline (0.1 µM, 100 nCi) in KRH for varying times (1, 3, 5, 10 and 20 minutes) and transport was quantified as described above.

Statistical analyses

Transport was compared employing one-way ANOVA with Dunnett's multiple comparisons post hoc test to see if the differences between the means were significant. Vector was used as the referent group for all post-hoc tests. For cell surface biotinylation studies, one-way ANOVA with Dunnett's multiple comparisons post hoc test was employed to test if the differences between the means were significant. Means were compared only within each fraction and the CHT1-WT value for that particular fraction was used as the referent group. For cell surface expression rescue experiments, untreated CHT1-WT value was used as the referent group for each fraction.

Supplementary Figures

Supp. Figure S1: A, Nerve conduction study trace Patient 2. Slow repetitive nerve stimulation (2 Hz) of the left spinal accessory nerve recording trapezial muscle. The resultant CMAPs (compound muscle action potentials) are low in amplitude (0.5 mV and less). There is a significant reproducible decrement at baseline (unmedicated) of 48-62% between the first and fourth stimulations, implicating a substantial neuromuscular junction transmission disorder. B, Nerve biopsy from Patient 2. Electron microscopy shows scattered enlarged axons with secondary myelin loss (black arrows) and accumulation of neurofilaments (open arrows) and other organelles. Similar ultrastructural observations have been described in cases of Giant Axonal Neuropathy.

Supp. Figure S2. Alignment of amino acid residues in the fourth cytosolic loop of CHT1 from various species.

Supp. Figure S3. A, Deglycosylation experiment using PNGase F or untreated samples. Lane "–" indicates mock deglycosylation, lane "+" indicates PNGase F treated samples. Black circle

indicates CHT1 carrying complex oligosaccharide, white circle shows core glycosylated CHT1, arrowhead indicates unglycosylated CHT1. B, Immunostaining of fixed HEK293 cells either expressing CHT1-WT or CHT1-S263FSer263Phe stained with anti-CHT1 antibody (green). Blue staining corresponds to DAPI and shows nuclei.

Supp. Table S1 Clinical characterization of families described with a lethal phenotype related to SLC5A7 mutations from the literature (Bauché et al; Wang et al; Pardal-Fernández et al. 2018) and this study.

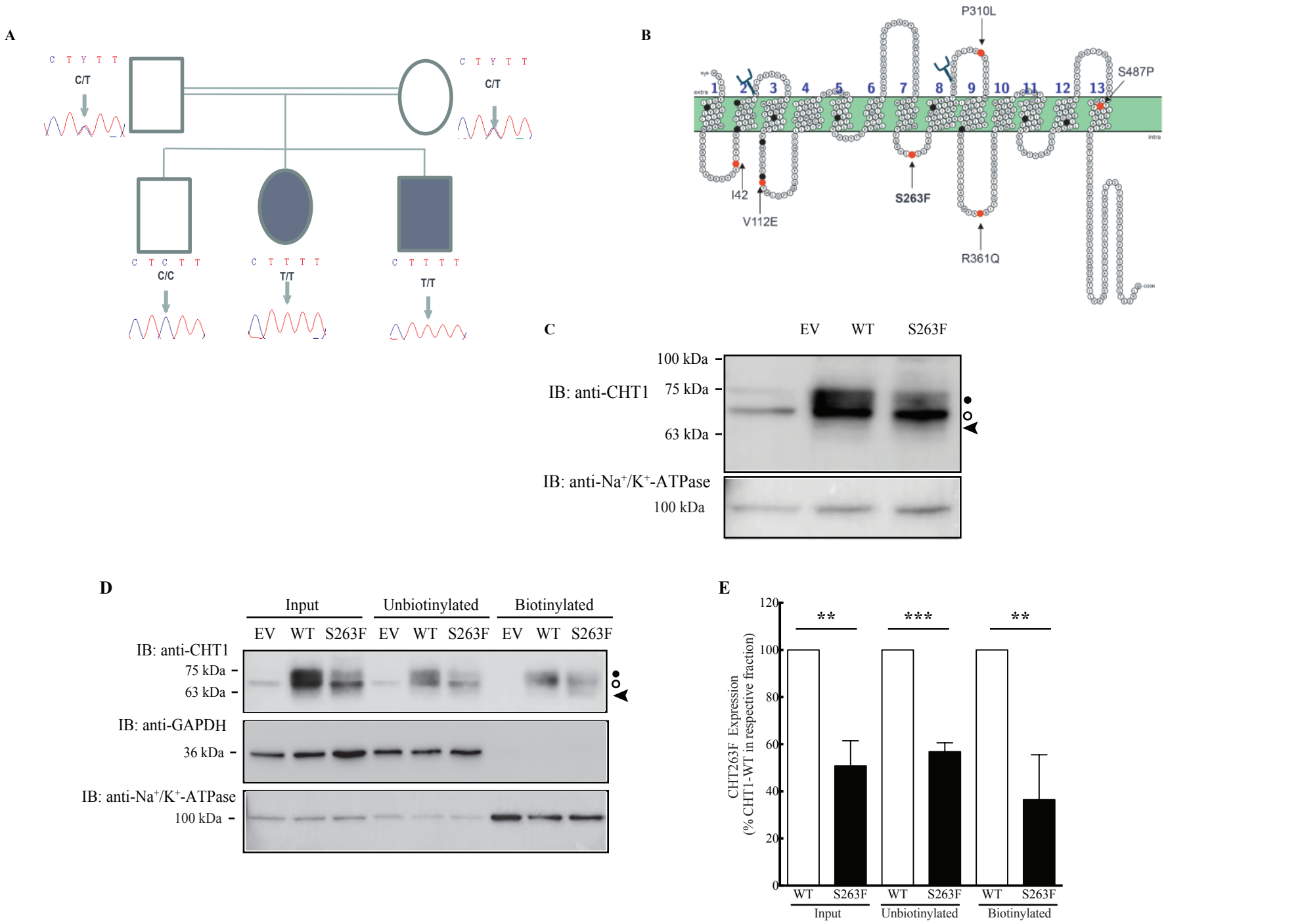

Figure 1 Banerjee et al.

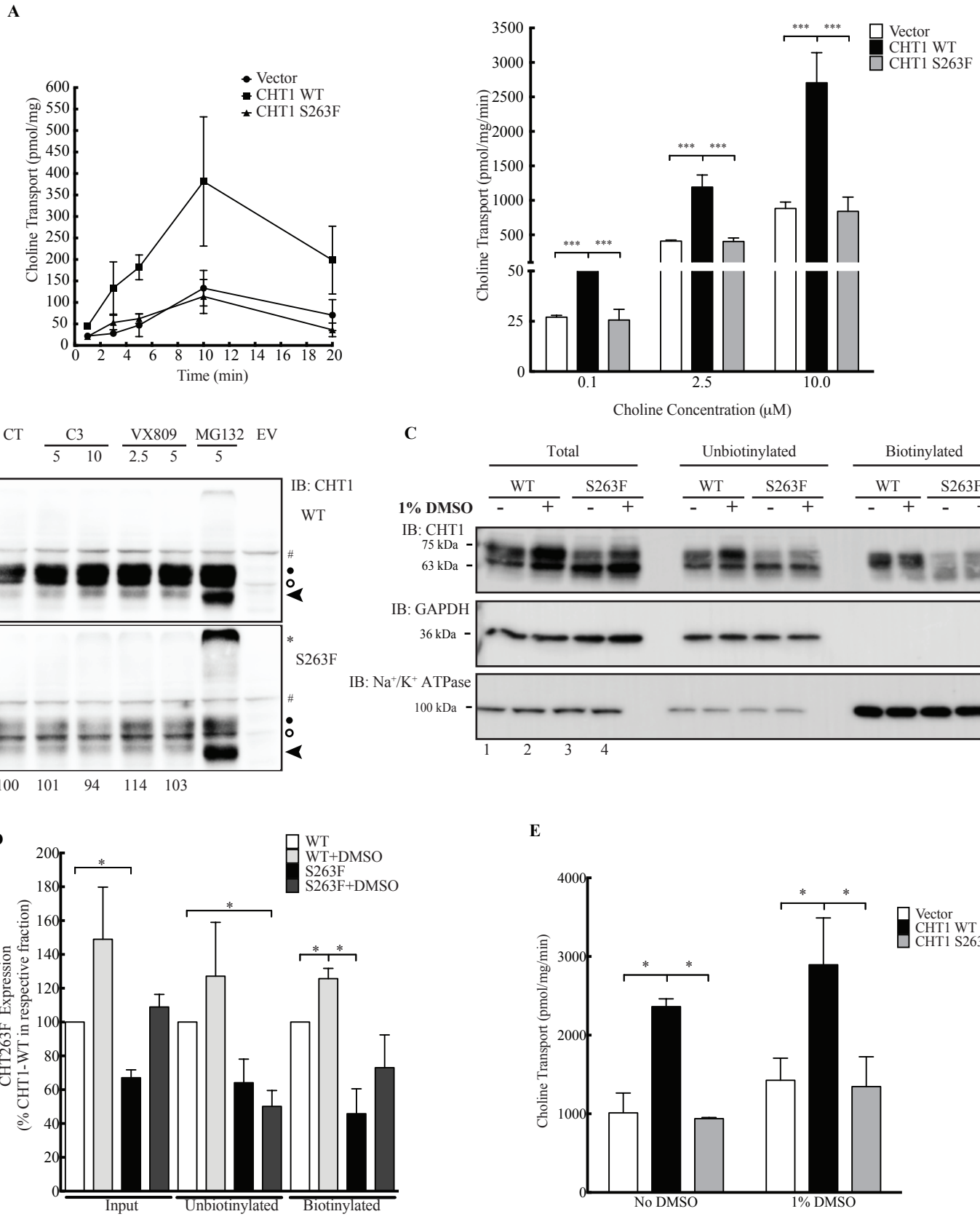

Figure 2 Banerjee et al.

The novel p.Ser263Phe mutation in the human high-affinity choline transporter 1 (CHT1/ *SLC5A7)* causes a lethal form of fetal akinesia syndrome.

Mayukh Banerjee*[,1], Denis Arutyunov*[,1], Daniel Brandwein[1], Cassandra Janetzki-Flatt[2], Hanna Kolski[4], Stacey Hume[2], Norma Jean Leonard[2,4], James Watt[4], Atilano Lacson[3], Monica Baradi[1], Elaine M. Leslie**[,1,3], Emmanuelle Cordat**[,1], Oana Caluseriu**[,2,4]

Supplementary Files

Detailed Materials and Methods

The Family

A Canadian consanguineous family of El Salvadorian ethnicity was evaluated in the neonatal period and found to have the same CMS-like disorder in two of their children, as shown in the pedigree (Figure 1A). The children displayed reduced prenatal movements, and arthrogryposis with elbow, wrist, and knee flexion, no pterygia and camptodactyly diagnosed at birth. The first child was a girl born at term who required resuscitation and intubation following the delivery. The diagnostic work up for hypotonia showed a normal female chromosomal complement, and normal genetic testing for Prader-Willi, spinal muscular atrophy, and myotonic dystrophy type 1. There was a normal electroencephalogram (EEG), no structural brain anomalies on MRI, and nerve conduction studies/electromyography (EMG) were suggestive of a myasthenia gravis-like pattern (decrement with slow repetitive nerve stimulation). Further clinical genetic testing available at the time showed no pathogenic variants in the rapsyn, alpha and epsilon subunits of the acetylcholine receptor gene, and the COLQ gene by sequencing. She remained areflexic, with profound hypotonia, and was ventilator dependent (requiring supplemental manual ventilation due to acute episodes of decompensation). There was no clinical improvement with the use of pyridostigmine, 3,4-diaminopyridine, fluoxetine, and salbutamol. At 5 months of age, the family decided to withdraw care. Five years later, a brother was born at 36 weeks gestation following a pregnancy characterized by lack of fetal movements and polyhydramnios. His neonatal presentation was similar to his sister; he required neonatal resuscitation and was ventilator-dependent, had profound hypotonia and minimal muscle power against gravity. Nerve conduction studies (Supp. Figure S1A) showed severe axonal motor and sensory polyneuropathy with neuromuscular junction dysfunction, and brain MRI was normal. A nerve biopsy showed primary axonopathy with giant axons and secondary myelin loss (Supp. Figure S1B). A course of pyridostigmine did not improve his presentation. He had two rounds of aspiration

pneumonia and withdrawal of care was decided at 1.5 months of age. Parents were reportedly healthy with no congenital anomalies or neurodevelopmental disorders.

A single nucleotide polymorphism (SNP) clinical array was performed for the purpose of identifying areas of homozygosity shared by the two affected siblings. These were: hg19: 12q11q13.13 (chr12:37857750-52353578); 19q13.11q13.41 (chr19:34168272-51640321); 2q11.1q14.1 (chr2:95341387-115179913); 3p21.31p21.1 (chr3:46726738-53002150); 9q21.13q21.32 (chr9:78190522-84727196). None of the 18 CMS genes known at the time, majority of them recessive, (Hantai et al., (2013)) were located within the homozygosity regions identified. Further, the family was offered next generation sequencing studies on a research basis upon signing informed written consent approved by the University of Alberta human research ethics board (Protocol 00043169) for the unaffected parents, the affected children and an unaffected brother. At the end of the study, in view of additional CMS genes discovered in the meantime, the exome data obtained previously on the two affected siblings was again screened for variants in all 30 genes reported (McMacken et al., (2017)). A variable number of SNPs were identified in the majority of the genes in both patients, with the exception of a heterozygous MYO9A variant in patient 2, and a heterozygous COLQ splicing variant in patient 1. Of note, both MYO9A and COLQ are known to be responsible for autosomal recessive forms of CMS, and therefore these variants were not considered to contribute to the phenotype in our patients.

Whole exome sequencing studies

Genomic DNA from the two affected patients underwent whole exome sequencing (WES) performed by Macrogen Inc. using Agilent's SureSelect 51 Mb enrichment kit at 100X average on-target depth coverage. Sequencing was completed on an Illumina HiSeq 2000 using 100-bp paired-end sequencing method and a target coverage of 99%. The reads were mapped against UCSC hg19 (http://genome.ucsc.edu/), using BWA (http://bio-bwa.sourceforge.net/) and SAMTOOLS (http://samtools.sourceforge.net/). The ~75 000 variants per patient were filtered as follows: minor

allele frequency of 1% or higher in dbSNP135 and 1000 genome, and variants in the known CMS genes to date without an identified pathogenic variant. Subsequently, we proceeded to analyze data under an autosomal recessive model of inheritance by focusing the analysis on the regions of homozygosity identified by SNP array.

Site-directed mutagenesis

The human CHT1-WT cDNA was a gift from Randy Blakely (Addgene, plasmid # 15766) (Apparsundaram et al., (2000)). The single nucleotide variant c.788C>T (p.Ser263Phe) was generated by site-directed mutagenesis. Briefly, the human CHT1 cDNA was cloned into the pLVX-IRES-Hygromycin B (Hyg) vector (Clontech) using BamHI restriction sites flanking the CHT1 cDNA. After confirmation of the successful cloning by Sanger sequencing, the construct bearing human CHT1-wild-type (WT) cDNA was amplified using the Q5 site-directed mutagenesis kit (New England Biolabs) with mutagenic primers containing the desired variant (hCHT1 Ser263Phe Forward: AGG GTT CTC TTT TCT TCC TCA G; hCHT1 Ser263Phe Reverse: CTG AAA GTA TGC TTG CCA TG). The resulting cDNA was sequenced to confirm the presence of the variant (The Applied Genomics Core, University of Alberta, Edmonton, Canada).

Cell Culture

HEK293 cells (Clontech) were grown in complete medium [Dulbecco's Modified Eagle's Medium (DMEM) (Gibco) supplemented with 10% fetal bovine serum (FBS) (Sigma-Aldrich), 100 units/ml of penicillin and 100 µg/mL of streptomycin (ThermoFisher Scientific)] at 37°C in a humidified incubator with 5% CO2. To express human CHT1 in mammalian cells, we used a lentiviral infection process, followed by selection to obtain HEK293 cells stably expressing either CHT1-WT or CHT1-Ser263Phe. First, CHT1-WT or CHT1-Ser263Phe cDNA in pLVX-IRES-Hyg was transiently transfected in HEK293 cells using the single shot packaging kit (Clontech) and the supernatant containing the viruses was collected 48 hours later. After filtering through a 0.45 µm filter, the cell

supernatant was used to transduce new HEK293 cells in the presence of 8 µg/ml polybrene (Sigma) and CHT1-stably expressing cells were selected in complete growth medium supplemented with 0.2 mg/ml Hygromycin B (Thermo Scientific).

Immunoblot

Confluent HEK293 cells expressing CHT1-WT and CHT1-Ser263Phe were lysed in PBS containing 1% Triton X-100 and protease inhibitors [Complete™ Mini EDTA-free (Roche)]. Total protein concentration was measured using the BCA (bicinchoninic acid) protein assay kit (Pierce). Total proteins (20 µg) were subjected to SDS-PAGE, transferred onto a PVDF membrane (Millipore) and membranes were then blocked with 3% skim milk powder (BioBasic) in Tris-buffered saline with 0.1 % Tween 20 (TBST) for 1 hr. Membranes were incubated with anti-CHT1 rabbit polyclonal antibody (ABN458, 1:2500) (Millipore) in TBST containing 1% skim milk followed by anti-rabbit HRP-conjugated secondary antibody (1:10,000) (GE Healthcare). Proteins on the blots were detected with Clarity Western chemiluminescent detection reagent (Bio-Rad) and bands visualized using ChemiDoc MP Imaging System (BioRad). Membranes were subsequently re-probed with monoclonal anti-mouse β-actin antibody (1:20,000, Origen) in 1% BSA TBST followed with HRP-conjugated anti-mouse secondary antibody (1:15,000, GE Healthcare) in 1% BSA TBST. Relative band intensities were determined using the freeware ImageLab (Bio-Rad).

For rescuing CHT1-Ser263Phe, 50% confluent cells were incubated with complete medium containing 0.2 mg/ml hygromycin and C3 (kind gift from Dr. Gergely Lukacs, McGill University), VX809 (Selleckchem) or DMSO at the indicated concentrations. Cells were subsequently grown for 24 hours at 37°C under standard conditions. Cells were then lysed on ice in PBS containing 1% Triton-X-100 (Fisher Scientific) and CompleteMini EDTA-free Protease Inhibitor Cocktail (Roche). Lysate protein concentrations were determined using a BCA Protein Assay kit (Pierce) and the samples were subjected to immunoblot, as described above.

Immunofluorescence

HEK293 cells expressing CHT1-WT, CHT1-Ser263Phe or empty vector were seeded on 6 well plates with poly-L-lysine coated coverslips. Cells were fixed with 4% paraformaldehyde in PBS, washed with PBS containing 100 mM glycine, permeabilized with 0.2% Triton X-100 in PBS, and blocked with 1% BSA in PBS. Coverslips were then incubated with rabbit anti-CHT1 polyclonal antibody (1:500, Millipore) in 1% BSA in PBS for 30 min, washed and incubated with goat anti-rabbit antibody conjugated with Alexa 488 (1:500, GE Healthcare) in 1% BSA in PBS. DAPI (Thermo Scientific) was used to stain nuclei. The coverslips were then mounted on slides with DAKO mounting solution. Image acquisition was done with an Olympus IX81 microscope equipped with a Nipkow spinning disk optimized by Quorum Technologies (Guelph, ON, Canada) and a 63X oil objective.

Cell surface biotinylation

HEK293 cells expressing CHT1-WT, CHT1-Ser263Phe or empty vector were seeded on 6 well plates. Forty-eight hours post-seeding, the cells were incubated with or without 1% DMSO in complete medium for 24 hours. The cells were subsequently subjected to cell surface biotinylation, as described previously (Banerjee et al., (2016)), with minor modifications. Following incubation with membrane impermeant EZ-Link biotinylation reagent (Thermo Scientific, Rockforl, IL) and lysis as described previously, total protein levels were measured. An aliquot of the lysate was saved (total fraction) and 450 µg of each lysate was subsequently incubated with 140 µL streptavidin beads for 1 hour on a rocker at 4°C. Following centrifugation, the supernatant was collected, and an aliquot kept as the unbiotinylated fraction. After washing, the beads were resuspended in 50 µl of 2X Laemmli buffer and incubated at room temperature for 30 min. The eluted biotinylated proteins were subsequently collected by centrifugation (biotinylated fraction) and 25 µl loaded for immunoblot along with 2.5 µg of total fraction and a matched volume of unbound fraction per well. In addition to CHT1, the blots were probed for cytosolic GAPDH to ensure cell membrane integrity was intact during the biotinylation procedure [mouse monoclonal anti-GAPDH 6C5 (1:10,000); Santa Cruz Biotechnology,

Dallas, TX], and for Na^+/K^+ATPase as a loading control [mouse monoclonal anti Na^+/K^+ATPase H-3 (1:10,000); Santa Cruz Biotechnology, Dallas, TX]. Since the Na^+/K^+ATPase is present in both the unbound and biotinylated fractions, each fraction was normalized for loading only within that particular fraction.

Choline uptake assay

HEK293 cells stably expressing empty vector, CHT1-WT or CHT1-Ser263Phe were seeded on poly-L-lysine coated 6 well plates at a density of 0.8 x 106 cells/well in a total volume of 2 ml. Choline uptake was measured based on a previously described method (Okuda and Haga, (2003)) with modifications. Briefly, after 48 hours, the cells were washed twice with 1.5 ml of warm (37°C) Krebs-Ringer's-HEPES (KRH) buffer (130 mM NaCl, 1.3 mM KCl, 2.2 mM $CaCl_2.2H_2O$, 1.2 mM $MgSO_4.7H_2O$, 1.2 mM KH_2PO_4, 10 mM HEPES, 10 mM glucose, pH 7.40). The cells were then pre-incubated at 37°C with KRH buffer for 10 minutes, next replaced with 1 ml of KRH containing [^{3}H]-choline (choline chloride, [methyl-^{3}H], 78.3 Ci/mmol, Perkin Elmer) (0.1, 2.5 or 10 µM, 100 nCi/ml) and incubated at 37°C for 5 min. Cells were next washed three-times with ice-cold KRH buffer and lysed using 750 µl of 1% SDS in water. Transport of [^{3}H]-choline was quantified using a liquid scintillation counter (Beckman model LS6000IC). Transport activity was normalized against the total protein concentration in each well.

For the time course experiment, cells were incubated with [^{3}H]-choline (0.1 µM, 100 nCi) in KRH for varying times (1, 3, 5, 10 and 20 minutes) and transport was quantified as described above.

Statistical analyses

Transport was compared employing one-way ANOVA with Dunnett's multiple comparisons post hoc test to see if the differences between the means were significant. Vector was used as the referent group for all post-hoc tests. For cell surface biotinylation studies, one-way ANOVA with Dunnett's multiple comparisons post hoc test was employed to test if the differences between the

means were significant. Means were compared only within each fraction and the CHT1-WT value for that particular fraction was used as the referent group. For cell surface expression rescue experiments, untreated CHT1-WT value was used as the referent group for each fraction.

Supplementary Figures

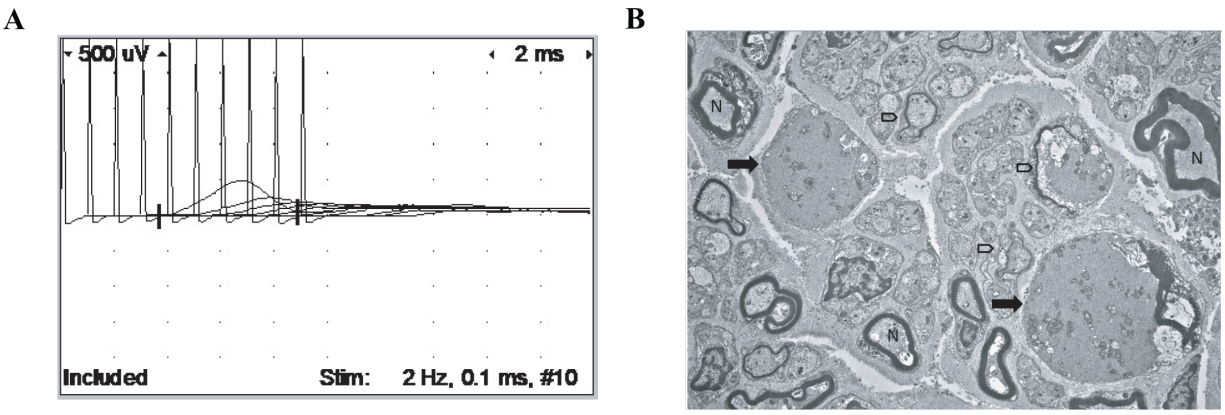

Supp. Figure S1: A, Nerve conduction study trace Patient 2. Slow repetitive nerve stimulation (2 Hz) of the left spinal accessory nerve recording trapezial muscle. The resultant CMAPs (compound muscle action potentials) are low in amplitude (0.5 mV and less). There is a significant reproducible decrement at baseline (unmedicated) of 48-62% between the first and fourth stimulations, implicating a substantial neuromuscular junction transmission disorder. B, Nerve biopsy from Patient 2. Electron microscopy shows scattered enlarged axons with secondary myelin loss (black arrows) and accumulation of neurofilaments (open arrows) and other organelles. Similar ultrastructural observations have been described in cases of Giant Axonal Neuropathy.

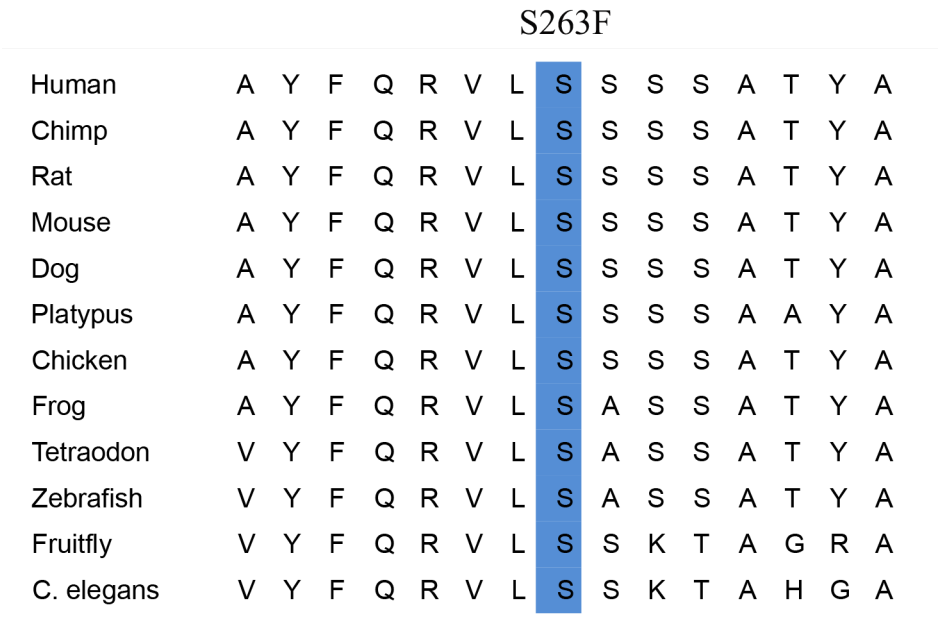

Supp. Figure S2. Alignment of amino acid residues in the fourth cytosolic loop of CHT1 from various species.

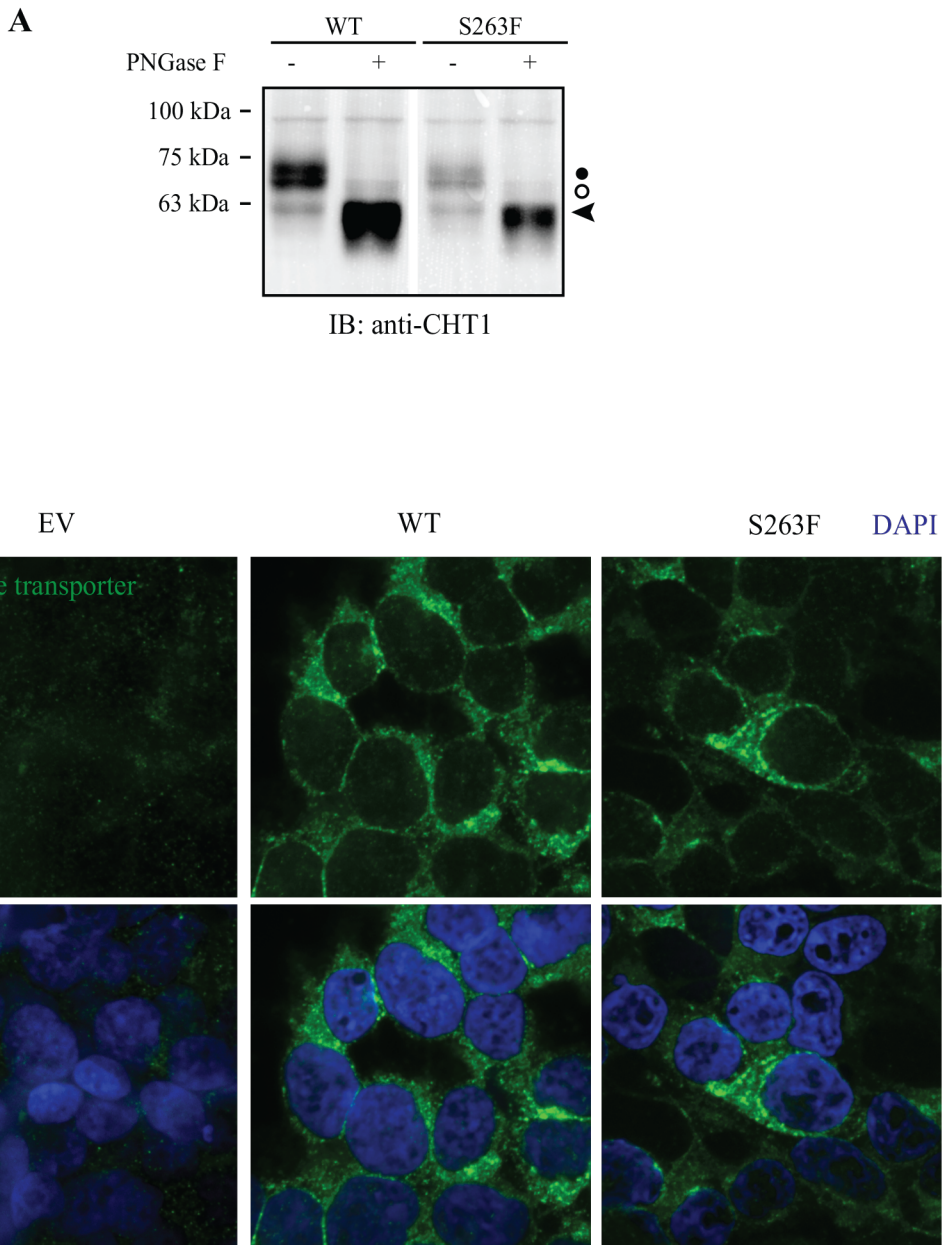

Supp. Figure S3. A, Deglycosylation experiment using PNGase F or untreated samples. Lane "–" indicates mock deglycosylation, lane "+" indicates PNGase F treated samples. Black circle indicates CHT1 carrying complex oligosaccharide, white circle shows core glycosylated CHT1, arrowhead indicates unglycosylated CHT1. B, Immunostaining of fixed HEK293 cells either expressing CHT1-WT or CHT1-Ser263Phe stained with anti-CHT1 antibody (green). Blue staining corresponds to DAPI and shows nuclei.

Supp. Table S1. Clinical characterization of families described with a lethal phenotype related to SLC5A7 mutations from the literature (Bauché et al. (2016); Wang et al. (2017); Pardal-Fernández et al. (2018)) and this study.

Pedigree	**Family 1 (Family 2, Bauché et al, 2016)**		**Family 2 (Family 2, Wang et al, 2017)**		**Family 3 (Pardal-Fernandez et al, 2018)**	**Our family**	
	Patient 1	**Patient 2**	**Patient 1**	**Patient 2**	**Patient 1**	**Patient 1**	**Patient 2**
Mutation	c.1082G>A, [p.R361Q]; c.123_126del, [p.I42*]		c.335T4A, [p.V112E]		c.929C>T' [P310L]; c.1459T>C , [p.S487P]	c.788C>T, [p.S263F]	
Gender	Male	Male	Female	Male	Male	Female	Male
Ethnicity	?		Hispanic?		?	San Salvadorian	
Age at latest presentation	Death at 10 days	Death at 15 days	Death at 11 months	Death at 6 months	?	Death at 5 months	Death at 2 months
Prenatal presentation	Polyhydramnios	Polyhydramnios	?	?	Reduced fetal movements	Polyhydramnios Reduced fetal movements	Polyhydramnios Reduced fetal movements
Presentation at birth	Delivery 34 wks, C/S W10th-25th Apgar 0^{1},4^{5},7^{10}	Delivery 40 wks W50th-75th; Apgar 2^{1},2^{5},4^{10};Active	Delivery 40 wks W 10$^{th;}$; Floppy	Delivery 38 wks	Delivery vaginal, induced at 39 wks; N growth parameters	Delivery 38 wks W 25th - 50th Apgar 2^{1},4^{5},5^{10}	Delivery 36+5/7 wks for BPP 2/8 W 50th

		movements Dysmorphism Arthrogryposis			Apgar 4^1, 6^5 Semiflex arms	Arthrogryposis	Apgar 3^1,4^5,4 Arthrogryposis
Neurological features	Seizures	Transitory eye opening Periods of coma	Severe hypotonia Bulbar insufficiency	Severe hypotonia	Severe hypotonia	Profoundly hypotonic	Profound hypotonia Developmental delay
Respiratory features	Intubated; in ICU	Intubated	Ventilator dependent	Ventilator dependent	Ventilator dependent	Ventilator dependent	Ventilator dependent
Other issues	Coagulation disorder	Hydrocele	Bowel perforation Seizure like episodes	Bowel perforation Seizure like activity	Seizure activity Encephalopathy	Feeding issues	
Neuroimaging	IVHIV	N	N	N		N	N
Treatment response			N/A	N/A	temporary	-	-

196